Stress invariant based elastoplastic damage modelling of unidirectional fiber reinforced composites

M.N. Rao, A.K. Bangaru, M.S. Meon, and K.-U. Schröder

Institute of Structural Mechanics and Lightweight Design, RWTH Aachen, Aachen, Germany

ABSTRACT

The primary objective of this work is to develop a model based on continuum damage mechanics and elastoplasticity theory for prediction of damage and failure in unidirectional fiber reinforced composites by the three-dimensional invariant approach. The invariant-based criteria utilize structural tensors concept that accounts for the orientation of fibers in the anisotropic material. The constitutive stress-strain relation for transversely isotropic materials is decomposed to fiber directional, transverse and shear parts to account for the formulation of respective failure criteria. The formulation is made under the assumption of fibers undergoing elastic deformations and the matrix elastoplastic deformations. A continuum damage based yield condition is defined for fiber, fiber/matrix interface failure with the assumption of associated plastic flow rule in the interface region. With the help of user defined subroutine, the combined fiber and fiber/matrix transverse debonding failure criteria have been implemented in the finite element software ABAQUS. Numerical simulations are performed for the open-hole coupon tension tests to validate the present damage model.

1 Introduction

The composite materials and structures owe to meet the desired characteristics based on different angles of ply orientation, sequencing of stacking and blending of various constituents. However, with this flexibility also comes to the complexity; in a sense, failure in these materials is characterized by the fact of inherent heterogeneity and anisotropy. Although there exist numerous failure models, often they are applicable for a particular type of loading or specific failure mechanism. Among them, Tsai-Wu [37], Tsail-Hill [9], Hashin [10], Puck and SchÃijrmann [30, 31], are the most widely used criteria.

In the framework of continuum damage mechanics (CDM), the damage phenomena such as fiber breakage, matrix cracking and fiber matrix interface debonding can be described by internal state (scalar) variables as long as the phenomena remain small in comparison to the problem size. It allows simple definitions for damage variables and accordingly provides directness in its applications. Initially, CDM was applied by Kachanov [15] to study the creep rupture of metals, and after that, it proved to be an excellent method to capture damage in composite laminates. Most of the CDM models employ a formulation where damage growth takes place according to the law of irreversible thermodynamics. Hild et al. [13, 14] and Burr et al. [6] studied fiber, and matrix breakage in ceramic-matrix fiber reinforced composites by introducing internal state variables. Matzenmiller et al. [22] developed a constitutive model correlating the effective elastic properties and damage of the material. Matzenmiller and colleagues defined a set of internal damage variables and a potential function and later derived dynamic equations for these variables. For tension and compression loading they considered separate damage states. Further, they studied the evolution of damage and its effect on stress-strain diagrams for uniaxial tension in the fiber direction. By combining continuum damage mechanics and micromechanics

Talreja et al. [35] proposed concepts for the analysis of mechanical behavior of unidirectional composites at a macroscopic level. The concepts were mainly applied for modeling crack in the transverse direction. Later some works also included the study at the microscopic level. For example, Megnis et al. [23] developed a model for damage prediction in fiber reinforced composites. With the help of an internal state variable, fiber breakage phenomenon was included in the model. Based on the strain applied, they determined stiffness degradation numerically in the composite and compared the data with experimental results.

Raghavan and Ghosh [32] work involved on a CDM model with damageable interfaces in composites. With the help of cohesive zone models, the interface debonding has been simulated. Based on micromechanical analysis of representative volume element damage variables along with evolution laws were determined. Hasan and Batra [11] employed three internal scalar variables relating each to fiber breakage, matrix cracking and fiber matrix interface debonding to study the evolution of damage in fiber-reinforced polymer composites. The authors used Voigt model in determining the dependence of material properties on the damage variables. They derived equations that characterize damage evolution and also developed a finite element code to model damage evolution in the composite. The tensile strength of the composites in relation to the fiber orientation angle and also the time histories of the evolution of damage variable was studied. Based on the CDM theory, Schapery [33], Murakami and Kamiya [24], and Hayakawa et al. [12], Tang et al. [36], Ristinmaa [5], Basu et al. [27], Brünig [3], Olsson and Maimi et al. [20, 21] presented stiffness degradation models and damage evolution models respectively with the help of second order or fourth order damage tensor. Particularly, Kwon and Liu [16], Schipperen [34], Maa and Cheng [19], Camanho et al. [7], Barbero and Vivo [2] constituted the thermodynamic models to represent the progressive failure properties and to interpret the stiffness degradation of composite laminates. One major drawback of these models is that they are all limited to the plane structures. Perreux et al. [29] and Ferry et al. [8] derived the constitutive relations of damaged materials using the CDM and fracture mechanics. Nevertheless, these models cannot elucidate the different failure modes of FRP composites as they defined only the single thermodynamic conjugate force and damage tensor. Furthermore, Perreux et al. [28], Liu and Zheng [18] described the damage evolution process with the help of three independent damage tensors each accounting for fiber breakage, matrix cracking and shear failure mode.

Nonetheless, it should be noted that the elastic/damage coupling constitutive model may be insufficient in order to precisely capture the damage initiation and evolution information of composite laminates. Hence, the damage/plasticity coupling nonlinear models are formulated to describe the interactive effect of the plastic deformations on the damage properties of the composite materials with regard to dissipative energy concept. This is usually accomplished by introducing the thermodynamic conjugate forces into the damage surfaces or plasticity potential functions. To simulate the behavior of composite laminates under uniaxial tension, Lin and Hu [17] proposed a nonlinear elasticity-plasticity/damage coupling constitutive model combined with a mixed failure criterion. By employing a homogenization method at the microscopic scale, Boutaous et al. [4] established an elastoplastic damage model. Combining CDM and classical thermodynamic theory, Barbero [1] proposed a damage/plasticity coupling model to predict the damage increments and permanent deformation. Nedjar et al. [25, 26] studied fiber damage, and fiber/matrix debonding by developing two different numerical models suitable to only specific failure modes explicitly and on single ply composites. The present work details both the fiber damage and fiber/matrix interface damage through potential functions, same as yield conditions, coupled with plastic flow rule to study the effect of damage evolution while on the other hand assuming elastic deformations in fibers. The developed 3D model is an extension of Nedjar et al. [25, 26] to study the different failure modes in one numerical model to suitable to evaluate the failure behavior of composite laminates.

2 Constitutive stress-strain relation and its decomposition

Transversely isotropic materials are characterized by symmetry about one direction referred to as principal material direction. Their properties remain unchanged by rotations/reflections from the planes orthogonal or parallel to this direction. Unidirectional fiber reinforced composites fall under this category; wherein the symmetry is exhibited along the direction of fibers. Let $\vec{l}$ denote the unit vector along the direction of fibers. Its components l_i $(i = 1, 2, 3)$ with respect to a fixed global cartesian basis say e_i $(i = 1, 2, 3)$ is construed as a continuous function of the position. Now one can construct a second order tensor called structural tensor by taking the tensor or dyadic product of the unit vector with itself as

$$\mathbf{L} = \vec{l} \otimes \vec{l}, \tag{1}$$

where L_{ij} $(i, j = 1, 2, 3)$ represents components of structural tensor and has the following important identities $\mathbf{L}^k = \mathbf{L},\ \mathrm{tr}\mathbf{L}^k = 1;\ k = 1, 2, ...n.$

2.1 Constitutive relation

A constitutive equation describes the response of a material to external disturbances such as applied fields or loads. The present work adopts the constitutive relation built on Integrity-basis formulation of transverse isotropy proposed by Spencer (1984). It consists of five basic invariants formed from strain tensor ε and structural tensor $\mathbf{L}$.

$$I_1 = \mathrm{tr}[\boldsymbol{\varepsilon}] \quad I_2 = \boldsymbol{\varepsilon} : \boldsymbol{\varepsilon} \quad I_3 = \det[\boldsymbol{\varepsilon}] \quad I_4 = \boldsymbol{\varepsilon} : \mathbf{L} \quad I_5 = \boldsymbol{\varepsilon}^2 : \mathbf{L}, \tag{2}$$

where $\det[\cdot]$ is the determinant operator. I_1, I_2 and I_3 are the classical invariants of isotropy and I_4 and I_5 arise due to the presence of the family of fibres. Let W denote the strain energy function and its quadratic nature with respect to the strain tensor results in an expression that is independent of the cubic invariant I_3, i.e., $W = W(I_1, I_2, I_4, I_5)$, given by

$$W = \frac{1}{2}\lambda I_1^2 + \mu_T I_2 + \alpha I_1 I_4 + 2(\mu_L - \mu_T) I_5 + \frac{1}{2}\beta I_4^2, \tag{3}$$

where λ, μ_T, μ_L, α, β are Lame-like elastic constants. μ_L and μ_T denote shear moduli on planes parallel to and normal to the fibres, respectively. The relation between the five Lame-like elastic constants and engineering parameters is given by

$$\begin{aligned}
\mu_L &= G_{LT} \\
\mu_T &= \frac{E_T}{2(1+\nu)} \\
\lambda &= \frac{\nu E_L + \nu_{LT}^2 E_T}{\frac{E_L}{E_T}(1-\nu^2) - 2\nu_{LT}^2(1+\nu)} \\
\alpha &= \frac{(\nu_{LT} + \nu\nu_{LT} - \nu)E_L - \nu_{LT}^2 E_T}{\frac{E_L}{E_T}(1-\nu^2) - 2\nu_{LT}^2(1+\nu)} \\
\beta &= \frac{(1-\nu^2)E_L^2 + \nu_{LT}^2 E_T^2 + (\nu - 2\nu_{LT}(1+\nu))E_L E_T}{E_L(1-\nu^2) - 2E_T\nu_{LT}^2(1+\nu)} - 4G_{LT} + \frac{E_T}{1+\nu}
\end{aligned} \tag{4}$$

where E, ν and G are youngs modulus, poisons ratio and shear modulus respectively, the subscript L refers to the fibers direction and T to the transverse plane normal to it.

With the definition of stress tensor as $\sigma = \frac{\partial W}{\partial \varepsilon}$ and by chain rule of differentiation, the constitutive relation is given by

$$\begin{aligned}\sigma =&\lambda \mathrm{tr}[\varepsilon]\mathbf{I} + \beta[\varepsilon : \mathbf{L}]\mathbf{L} + \alpha([\varepsilon : \mathbf{L}]\mathbf{I} + \mathrm{tr}[\varepsilon]\mathbf{L}) \\ &+ 2\mu_T \boldsymbol{\varepsilon} + 2(\mu_L - \mu_T)(\mathbf{L}\boldsymbol{\varepsilon} + \boldsymbol{\varepsilon}\mathbf{L}).\end{aligned} \tag{5}$$

wherein the following results are utilized

$$\frac{\partial I_1}{\partial \varepsilon} = \mathbf{I}, \quad \frac{\partial I_2}{\partial \varepsilon} = 2\boldsymbol{\varepsilon}, \quad \frac{\partial I_4}{\partial \varepsilon} = \mathbf{L}, \quad \frac{\partial I_5}{\partial \varepsilon} = \mathbf{L}\boldsymbol{\varepsilon} + \boldsymbol{\varepsilon}\mathbf{L} \tag{6}$$

2.2 Stress-strain tensors additive decomposition

The stress tensor can be additively split into three parts as

$$\boldsymbol{\sigma} = \mathbf{s} + p\mathbf{I} + r\mathbf{L}, \tag{7}$$

where $\mathbf{s}$ is the pseudo deviatoric stress tensor and the scalar stress terms p and r are determined by imposing the following conditions:

$$\mathrm{tr}[\mathbf{s}] = 0, \quad \mathbf{s} : \mathbf{L} = 0 \tag{8}$$

It results in the following equations and $\mathbf{s}$ is directly obtained from the pseudo-deviatoric fourth-order projection tensor $\mathcal{P}$ as $\mathbf{s} = \mathcal{P} : \boldsymbol{\sigma}$

$$p = \frac{1}{2}[\boldsymbol{\sigma} : (\mathbf{I} - \mathbf{L})], \tag{9}$$

$$r = \frac{1}{2}[\boldsymbol{\sigma} : (3\mathbf{L} - \mathbf{I})]. \tag{10}$$

For single family of fibers and three-dimensional space, the pseudo projection tensor is given by the relation

$$\mathcal{P} = \mathcal{I} - \frac{1}{2}\mathbf{I} \otimes \mathbf{I} - \frac{3}{2}\mathbf{L} \otimes \mathbf{L} + \frac{1}{2}(\mathbf{L} \otimes \mathbf{I} + \mathbf{I} \otimes \mathbf{L}) \tag{11}$$

An analogous additive split terms for the strain tensor can be written as

$$\boldsymbol{\varepsilon} = \mathbf{e} + \chi\mathbf{I} + \psi\mathbf{L}, \tag{12}$$

where $\mathbf{e}$ is the pseudo deviatoric strain tensor given by $\mathbf{e} = \mathcal{P} : \varepsilon$, and the scalar strain quantities χ and ψ are similarly determined by imposing the conditions: $\mathrm{tr}[\mathbf{e}] = 0, \quad \mathbf{e} : \mathbf{L} = 0$.

Now substituting stress-strain additive terms in the constitutive relation (6) yields the following individual relations

$$\mathbf{s} = 2\mu_T \mathbf{e} + 2(\mu_L - \mu_T)[\mathbf{L}\mathbf{e} + \mathbf{e}\mathbf{L}], \tag{13}$$

$$p = (\lambda + \mu_T)\mathrm{tr}[\varepsilon] + (\alpha - \mu_T)[\varepsilon : \mathbf{L}], \tag{14}$$

$$r = (\alpha - \mu_T)\mathrm{tr}[\varepsilon] + (\beta + 4\mu_L - \mu_T)[\varepsilon : \mathbf{L}]. \tag{15}$$

In much simpler form, the above relations can be rewritten with the help of constants as

$$\mathbf{s} = \mathcal{C}_s : \varepsilon, \quad p = \kappa_1 \mathrm{tr}[\varepsilon] + \kappa_2[\varepsilon : \mathbf{L}], \quad r = \kappa_2 \mathrm{tr}[\varepsilon] + \kappa_3[\varepsilon : \mathbf{L}]. \tag{16}$$

where $\mathcal{C}_s$ represents pure shear elasticity moduli given by

$$\mathcal{C}_s = 2\mu_T \mathcal{I} + 2(\mu_L - \mu_T)\mathcal{I}_F, \tag{17}$$

with $\mathfrak{J}_F$ representing fiber direction dependent fourth-order tensor having the identity $\mathfrak{J}_F : \mathbf{e} = \mathbf{Le} + \mathbf{eL}$, its component form is expressed as

$$(\mathfrak{J}_F)_{ijkl} = \frac{1}{2}(l_i l_k \delta_{jl} + l_i l_l \delta_{jk} + l_j l_l \delta_{ik} + l_k l_i \delta_{il}) \tag{18}$$

and

$$\kappa_1 = \lambda + \mu_T, \quad \kappa_2 = \alpha - \mu_T, \quad \kappa_3 = \beta + 4\mu_L - \mu_T. \tag{19}$$

3 Damage modeling in fiber and its normal direction

In order to model damage in unidirectional fiber reinforced composites, it is of primary importance to differentiate between longitudinal direction fiber dominated failures and transverse direction matrix dominated failures. Within the scope of continuum damage mechanics, we choose internal variable to represent damage and couple them with the simple yet efficient yield criterion in respective directions.

3.1 Modeling of fiber damage

For longitudinal fiber breakage, a strain invariant that gives strain history along the direction of fibers is used for formulating the yield criterion. In simplest form, stresses coupling the damage variable can be written as

$$\boldsymbol{\sigma} = (1-d)\boldsymbol{\sigma}_0, \tag{20}$$

where $\boldsymbol{\sigma}_0$ is the effective undamaged stress tensor given by (6) and the scalar d is the internal fiber damage variable with its value ranging from 0 to 1. So,

$$d = \begin{cases} 0 & \text{if fibers are undamaged} \\ 1 & \text{if fibers are completely damaged} \end{cases} \tag{21}$$

This damage variable is coupled locally to the strain history along the fibers through the invariant I_4 which is nothing but the projection $[\boldsymbol{\varepsilon} : \mathbf{L}] = \vec{l}.\boldsymbol{\varepsilon}\vec{l}$ along the plane of fibers. Hence, I_4 constitutes an excellent parameter to govern the fiber damage mode. For this, we choose the following criterion:

$$\mathcal{G}(d; I_4) = (1-d)^m I_4 - \varepsilon_F \leq 0 \tag{22}$$

where $\varepsilon_F > 0$ is the strain-like initial damage threshold and the constant parameter $m > 0$ controls the hardening/softening response.

Above criterion implies that damage evolution takes place when the strain along the fibers reaches the critical value $\varepsilon_F/(1-d)^m$. Here, the value obtained when $d = 0$ is the initial threshold ε_F. We set the following simple rule for the evolution of damage:

$$\begin{aligned} & d = \dot{\gamma} \\ & \gamma \geq 0, \quad \mathcal{G}(d; I_4) \leq 0, \quad \gamma\mathcal{G}(d; I_4) = 0 \end{aligned} \tag{23}$$

where γ is a multiplier satisfying Kuhn-Tucker loading/unloading conditions (Simo and Hughes).

In the context of the finite element, the condition (5.3) is realized locally at each integration point. Let t_n and t_{n+1} denote current time and time increment respectively. For the time interval $[t_n, t_{n+1}]$ with $\Delta t = t_{n+1} - t_n$, the damage value d_n is known at time t_n. Now, one has to update the variable d_{n+1} at time t_{n+1}. This is accomplished from the known strain tensor ε_{n+1} (strain driven solution) during the iterative process. Also, one can compute the fiber strain $I_{4_{n+1}}$.

Here, we use trial predictor/damage corrector scheme. At first, the criterion is evaluated at the trial state $d = d_n$ and $I_4 = I_{4_{n+1}}$ as

$$\mathcal{G}^{tr}_{n+1} \equiv \mathcal{G}(d_n; I_{4_{n+1}}) = (1-d)^m I_4 - \varepsilon_F. \tag{24}$$

Now, if $\mathcal{G}^{tr}_{n+1} \leq 0$, the trial state is possible and therefore we set $d_{n+1} = d_n$. Otherwise, if $\mathcal{G}^{tr}_{n+1} > 0$, the trial state is not possible and the correction is performed by solving $\mathcal{G}_{n+1} \equiv \mathcal{G}(d_{n+1}; I_{4_{n+1}}) = 0$ for d_{n+1}. Thus, we get

$$d_{n+1} = 1 - \left(\frac{\varepsilon_F}{I_{4_{n+1}}}\right)^{1/m}. \tag{25}$$

The strain softening behavior of fibers provides no unique solution. This is due to the dependency of strain on element (mesh) size. In order to avoid this, a viscoelastic damage model obtained from Duvaut-Lions type regularization (Duvaut and Lions 1972) is employed in the present work.

Let d denote the inviscid solution of the damage problem (23) and (24) and we now introduce the visco-damage variable d^v as

$$\dot{d^v} = \frac{1}{\eta}(d - d^v), \tag{26}$$

where η is a fluidity parameter. By an implicit backward-Euler scheme, the above equation is discretized as

$$d^v_{n+1} = \frac{\eta d^v_n + \Delta t d_{n+1}}{\eta + \Delta t} \tag{27}$$

with $\Delta t = t_{n+1} - t_n$ and d_{n+1} being the inviscid solution obtained from (26). The fluidity parameter η, in general, is set to a small value to avoid unstable solutions.

3.2 Modeling of damage in transverse direction to fibers

In this case the damage referred to as debonding is primarily caused by the tensile stresses that are normal to the fibers. Recall the definition of the scalar stress term p, the projection $[\boldsymbol{\sigma} : \mathbf{L}]$ corresponds to stress along the fibers whereas the complementary projection $[\boldsymbol{\sigma} : (\mathbf{I} - \mathbf{L})]$ gives a measure of the stress state normal to the fibers, i.e., transverse stresses. Hence, the term p forms a critical parameter in this debonding process.

So we define a p-dependent yield criterion together with a flow rule that describes the way debonding takes place. Here, the total strain tensor is additively split into elastic ε^e and plastic ε^p parts. Let the yield criterion be

$$\mathcal{G}(p, \xi) = p - p_y \exp[-K\xi] \leq 0, \tag{28}$$

where ξ is the strain-like internal variable characterizing isotropic hardening, $p_y > 0$ is the transverse flow stress and the non-dimensional parameter K controls hardening $(K < 0)$ or softening $(K > 0)$ regime.

Also, we consider an associated plastic flow rule with the following evolution equations:

$$\begin{aligned} \dot{\varepsilon^p} &= \gamma \frac{\partial \mathcal{G}}{\partial \boldsymbol{\sigma}} \equiv \frac{\gamma}{2}(\mathbf{I} - \mathbf{L}), \\ \dot{\xi} &= \gamma, \\ \gamma \geq 0, &\quad \mathcal{G}(p, \xi) \leq 0, \quad \gamma \mathcal{G}(p, \xi) = 0. \end{aligned} \tag{29}$$

where γ is the consistency parameter that satisfies the Kuhn-Tucker loading/unloading conditions. Now, one can construct the following properties:

$$\mathrm{tr}[\dot{\varepsilon^{\mathrm{p}}}] = \gamma \quad [\varepsilon^p : \mathbf{L}] = 0 \quad \dot{\mathbf{e}^p} = 0 \tag{30}$$

where $\mathbf{e}^p$ is the plastic-pseudo deviatoric part of ε^p.

From these relations, the split terms of the stress-strain constitutive relation (17) become

$$\begin{aligned} &\mathbf{s} = \mathfrak{C}_s : \mathbf{e}, \\ &p = \kappa_1(\mathrm{tr}[\varepsilon] - \mathrm{tr}[\varepsilon^{\mathrm{p}}]) + \kappa_2[\varepsilon : \mathbf{L}], \\ &r = \kappa_2(\mathrm{tr}[\varepsilon] - \mathrm{tr}[\varepsilon^{\mathrm{p}}]) + \kappa_3[\varepsilon : \mathbf{L}], \end{aligned} \tag{31}$$

As it can be observed that plastic straining affects only the scalar terms p and t while the behavior is elastic in pure shear. Here the plastic strain update is done by the use of simple elastic predictor/plastic corrector algorithmic scheme.

In the context of the finite element, the plastic flow rule (5.14) is realized locally at each integration point. Let t_n and t_{n+1} denote current time and time increment respectively. For the time interval $[t_n, t_{n+1}]$ with $\Delta t = t_{n+1} - t_n$, $\varepsilon^p]_n$ and ξ_n are known at time t_n. By use of the backward-Euler scheme, the evolution equations (5.14) are discretized in incremental forms as:

$$\begin{aligned} \mathrm{tr}[\varepsilon^{\mathrm{p}}_{\mathrm{n+1}}] &= \mathrm{tr}[\varepsilon^{\mathrm{p}}_{\mathrm{n}}] + \Delta\gamma, \\ \xi_{n+1} &= \xi_n + \Delta\gamma, \\ \Delta\gamma \geq 0, \quad \mathcal{G}_{n+1} &\leq 0, \quad \Delta\gamma\mathcal{G}_{n+1} = 0. \end{aligned} \tag{32}$$

where $\Delta\gamma = \gamma\Delta t$ and $\mathcal{G}_{n+1} \equiv \mathcal{G}(p_{n+1}, \xi_{n+1})$. At first, the criterion is evaluated at trial state as $\mathcal{G}^{tr}_{n+1} \equiv \mathcal{G}(p^{tr}_{n+1}, \xi_n)$ with

$$p^{tr}_{n+1} = \kappa_1(\mathrm{tr}[\varepsilon_{\mathrm{n+1}}] - \mathrm{tr}[\varepsilon^{\mathrm{p}}_{\mathrm{n}}]) + \kappa_2[\varepsilon_{n+1} : \mathbf{L}]. \tag{33}$$

Now, if $\mathcal{G}^{tr}_{n+1} \leq 0$, the trial state is possible and we set $\varepsilon^p_{n+1} = \varepsilon^p_n$ and $\xi_{n+1} = \xi_n$. Otherwise, if $\mathcal{G}^{tr}_{n+1} > 0$, the trial state is not possible and a correction is done by imposing the condition $\mathcal{G}_{n+1} = 0$ at time t_{n+1} and with the stress term as

$$p_{n+1} = p^{tr}_{n+1} - \kappa_1\Delta\gamma. \tag{34}$$

With (5.22) and $(5.20)_2$, it results in the following nonlinear equation in $\Delta\gamma$ which is solved by means of a Newton iteration scheme as

$$p^{tr}_{n+1} - \kappa_1\Delta\gamma - p_y \exp[-K\xi_n] \exp[-K\Delta\gamma] = 0. \tag{35}$$

Note that for $K = 0$, the case becomes perfect plasticity with simply the solution as

$$\Delta\gamma = \mathcal{G}_{n+1}/\kappa_1. \tag{36}$$

4 Simulation of combined fiber and fiber/matrix interface damage

A quasi-isotropic laminate with stacking sequence $[45/0/\text{-}45/90]_s$ is considered for analyzing both fiber damage and mode I debonding failure modes. The laminate has a central hole of diameter 6 mm

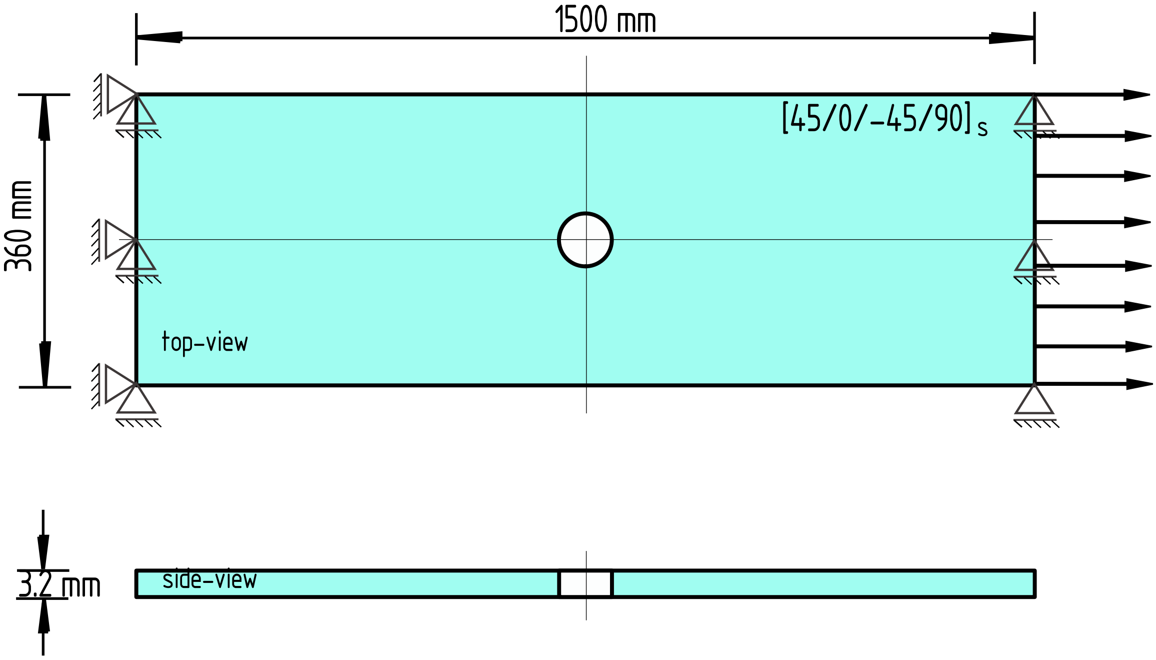

Figure 1: Composite laminate with centered hole subjected to tensile load

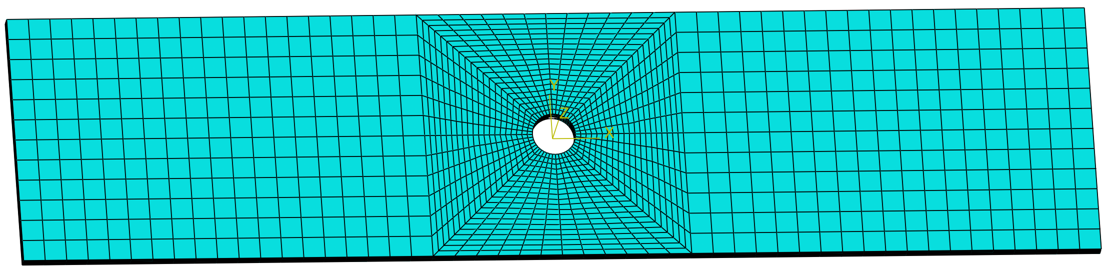

Figure 2: Mesh of open hole coupon

with length and width as 150 mm and 36 mm respectively. Its total thickness is 3.2 mm with an individual ply thickness of 0.2 mm. Its geometry along with boundary conditions is displayed in the Figure 1. As shown, one end of the laminate is fixed while the other the end is loaded with a displacement of 2 mm along global $\vec{e}_1$ axis. The material properties of the each ply are $E_L = 52$ GPa, $E_T = 8$ GPa,$G_{LT} = 3$ GPa, $\nu_{LT} = 0.28$, and $\nu = 0.34$. **Modeling:** The finite element model of the laminate is built with C3D8R elements. As stresses are concentrated around the notch region, mesh close to the notch is made fine. Mesh used for the analysis is shown in Figure 2. The yield parameters for fiber and mode-1 debonding are taken as $p_y = 15.0$ MPa, $K = 200$, $\varepsilon_F = 0.03$, and $m = 0.25$.

Result analysis: Figure 3 compares the analysis result with numerical and experimental observations of Liu et al. 2014. A peak stress value of 400 MPa is obtained for the laminate. After the peak load, the decline in stresses is attributed to the damages in matrix and fiber. The matrix and fiber damage evolutions in each ply of the laminate are shown in Figures 4-7. Because of the similar damage pattern observed in the bottom and the top sub-laminates, only damage in the four plies of the lower sub-laminate is illustrated. Each of the following figure shows damage initiation and final state of failure for both matrix and fiber along with the corresponding load states. From Figures (4-7), it is evident that matrix damage

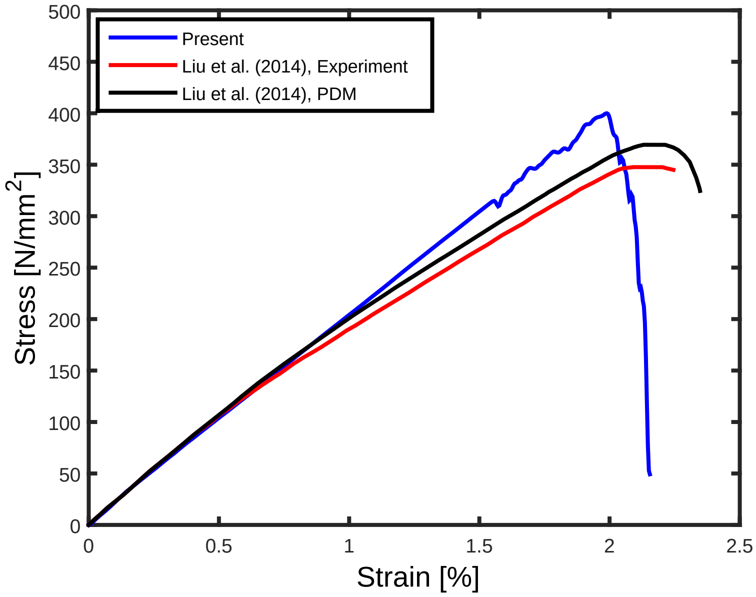

Figure 3: Stress vs. Strain plot for the tension test of the open hole laminate

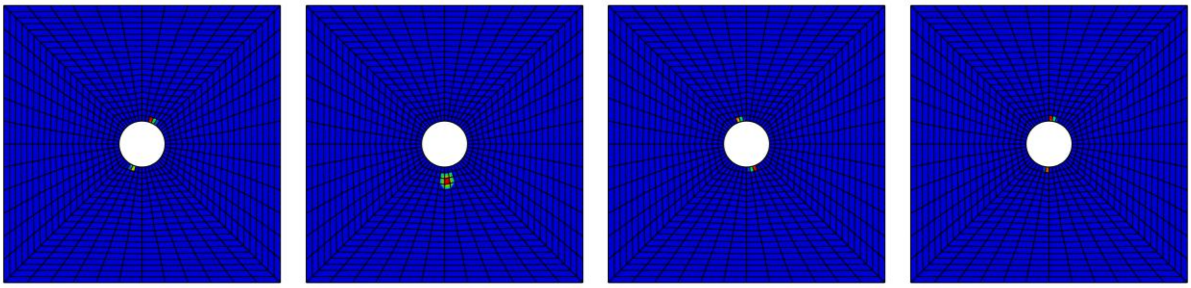

(a) 45°, at 910 N | (b) 0°, at 3898 N | (c) -45°, at 896 N | (d) 90°, at 592 N

Figure 4: Matrix damage initiation of the open hole laminate

in each ply first occurred at the notch edge and then extended on both sides following the path of the fiber direction. For 90° ply, the matrix damage initiated at a load value of 591.5 N which is less when compared to other angled plies. This is because Mode I causing transverse stresses are in the direction of the applied displacement and hence interface weakening occurs soon. While in 0° ply, applied displacement is along the direction of fibers. Thus, it requires a load of 3898 N to observe debonding. Analogously, for the very first fiber damagae intitation observed in 0° ply since the displacements/strains applied along the direction of the fibers. As expected there is no fiber damage in 90° ply even at the final failure load, where as the initiation fiber damage starts at slightly higher loads than the 0° ply.

5 Conclusions

The material constitutive stress-strain relation is disintegrated into three parts with each part representing the fiber directional, transverse and pure shear stresses in the material respectively. This split enabled in identifying the terms causing few dominant modes of failure. Concerning the failure of the fiber component, the fiber breakage in tension load case is presented with the help of the strain history data. For the matrix component failure, only interface, i.e., fiber/matrix debonding is introduced by employing

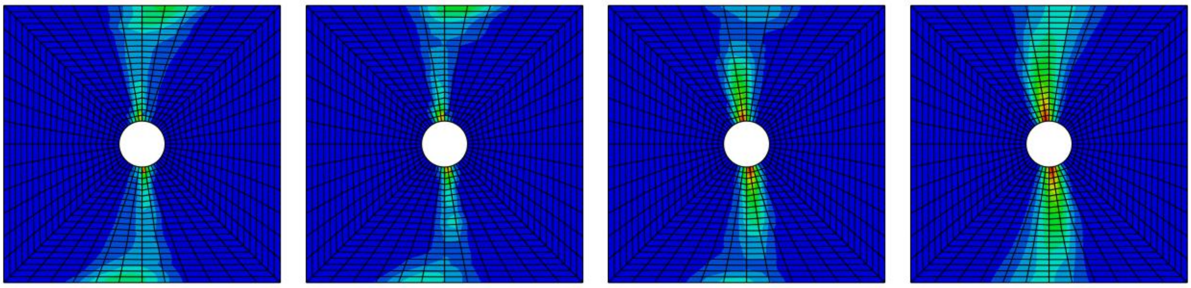

(a) 45° (b) 0° (c) −45° (d) 90°

Figure 5: Matrix damage at final failure of the open hole laminate

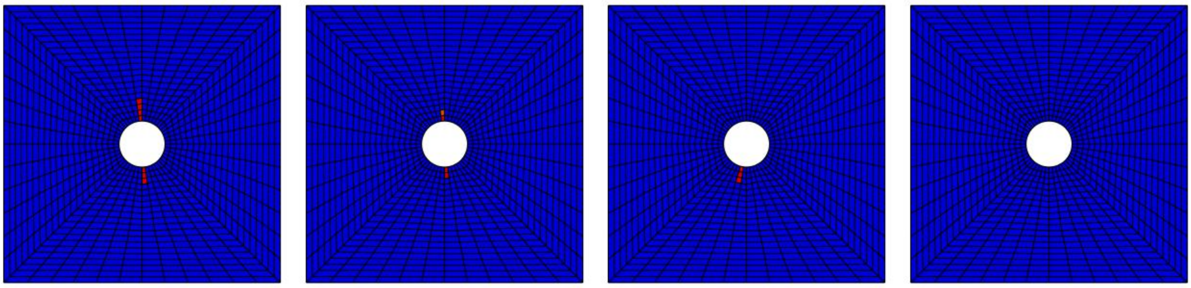

(a) 45°, at 21.94 kN (b) 0°, at 16.19 kN (c) −45°, at 21.36 kN (d) 90°, no fiber failure

Figure 6: Fiber damage initiation of the open hole laminate

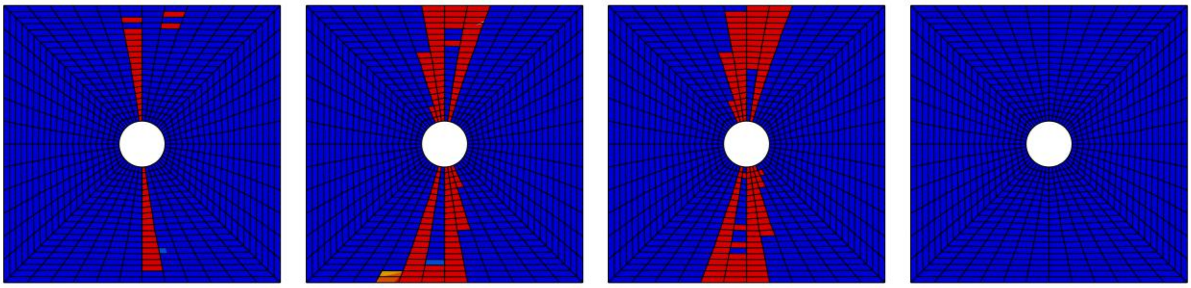

(a) 45° (b) 0° (c) −45° (d) 90°

Figure 7: Fiber damage at final failure of the open hole laminate

the invariants formed from the disintegrated terms and the structural tensor. The major possible case of transverse debonding combined with the fiber breakage is implemented at the local level within the context of a finite element method. Validation of the above approach is discussed by illustrating the failure of open-hole coupon under tensile loading, and the effectiveness of the present approach is discussed.

References

[1] E. J. Barbero. An inelastic damage model for the fiber reinforced laminates. *Journal of Composite Materials*, 36(8):941–962, 2002.

[2] E. J. Barbero and L. D. Vivo. A constitutive model for elastic damage in fiber reinforced pmc laminate. *International Journal of Damage Mechanics*, 10(1):73–93, 2001.

[3] S. Basu, A. M. Waas, and R. D. Ambur. Prediction of progressive failure in multidirectional composite laminated panels. *International Journal of Solids and Structures*, 44(9):2648–2676, 2007.

[4] A. Boutaous, B. Peseux, L. Gornet, and A. Belaidi. A new modeling of plasticity coupled with the damage and identification for carbon fiber composite laminates. *Composite structures*, 74(1):1–9, 2006.

[5] M. Bruenig. An anisotropic ductile damage model based on irreversible thermodynamics. *International Journal of Plasticity*, 19(10):1679–1713, 2003.

[6] A. Burr, F. Hild, and F. Leckie. Continuum description of damage in ceramic-matrix composites. *European Journal of Mechanics - A Solids*, 16:53–78, 1997.

[7] P. P. Camanho, P. Maimi, and C. G. Davila. Prediction of size effects in notched laminates using continuum damage mechanics. *Composite Science and Technology*, 67(13):2715–2727, 2007.

[8] L. Ferry, D. Perreux, J. Rousseau, and F. Richard. Interaction between plasticity and damage in the behavior of $[+\phi, -\phi]$ fiber reinforced composite pipes in biaxial loading (internal pressure and tension). *Composites Part B*, 29(6):715–723, 1998.

[9] H. T. Hahn and S. W. Tsai. *Introduction to composite materials*, volume 1. Technomic. Publishing Company (CRC Press), 1980.

[10] Z. Hashin. Failure criteria for unidirectional fiber composites. *Journal of applied mechanics*, 47(2):329–334, 1980.

[11] N. M. Hassan and R. C. Batra. Modeling damage in polymeric composites. *Composites Part B*, 39(1):66–82, 2008.

[12] K. Hayakawa, S. Murakami, and Y. Liu. An irreversible thermodynamics theory for elastic-plastic damage materials. *European Journal of Mechanics - A Solids*, 17(1):13–32, 1998.

[13] F. Hild, A. Burr, and F. A. Leckie. Fiber breakage and fiber pull-out of fiber-reinforced ceramic-matrix. composites. *European Journal of Mechanics - A Solids*, 13:731–749, 1994.

[14] F. Hild, A. Burr, and F. A. Leckie. Matrix cracking and debonding of ceramic-matrix composites. *International Journal of Solids and Structures*, 33(8):1209–1220, 1996.

[15] L. M. Kachanov. Time of the rupture process under creep conditions. *Ivz. Akad Nauk SSR Otd Tech Nauk*, 8:26–31, 1958.

[16] Y. W. Kwon and C. T. Liu. Study of damage evolution in composites using damage mechanics and micromechanics. *Composite structures*, 38(1-4):133–139, 1997.

[17] W. P. Lin and H. T. Hu. Nonlinear analysis of fiber-reinforced composite laminates subjected to uniaxial tensile load. *Journal of Composite Materials*, 36(12):1429–1450, 2002.

[18] P. F. Liu and J. Y. Zheng. Progressive failure analysis of carbon fiber/epoxy composite laminates

using continuum damage mechanics. *Material Science and Engineering A*, 485(1-2):711–717, 2008.

[19] R. H. Maa, J. H. Cheng, and A. CDM-based. failure model for predicting strength of notched composite laminates. *Composites Part B*, 33(6):479–489, 2002.

[20] P. Maimi, P. P. Camanho, and J. A. Mayugo. A continuum damage model for composite laminates: part i - constitutive model. *Mechanics of Materials*, 39(10):897–908, 2007.

[21] P. Maimi, P. P. Camanho, and J. A. Mayugo. A continuum damage model for composite laminates: part ii - computational implementation and validation. *Mechanics of Materials*, 39(10):909–919, 2007.

[22] A. Matzenmiller, J. Lublinear, and R. L. Taylor. A constitutive model for anisotropic damage in fiber-composites. *Mechanics of Materials*, 20:125–152, 1995.

[23] M. Megnis, P. Brondsted, S. A. Rehman, and T. Ahmad. Characterization of internal state variable for fiber fracture in ud composite. In S. Atluri and A. Tadeu, editors, *Advances in Computational and Experimental Engineering and Sciences*, pages 33–42. Tech Science Press, 2004.

[24] S. Murakami and K. Kamiya. Constitutive and damage evolution equations of elastic-brittle materials based on irreversible thermodynamics. *Internantional Journal of Mechanical Sciences*, 39(4):473–486, 1997.

[25] B. Nedjar. Plasticity-based modelling of fibre/matrix debonding in unidirectional composites. *Composite structures*, 108:41–48, 2014.

[26] B. Nedjar, N. Kotelnikova-Weiler, and I. Stefanou. Modeling of unidirectional fibrereinforced composites under fibre damage. *Composite structures*, 56:115–122, 2014.

[27] M. Olsson and M. Ristinmaa. Damage evolution in elasto-plastic materials response due to different concepts. *International Journal of Damage Mechanics*, 12(2):115–139, 2003.

[28] D. Perreux, D. Robinet, and D. Chapelle. The effect of internal stress on the identification of the mechanical behavior of composite pipes. *Composites Part A*, 37(4):630–635, 2006.

[29] D. Perreux and F. Thiebaud. Damaged elasto-plastic behavior of $[+\phi, -\phi]$ fiber reinforced composite laminates in biaxial loading. *Composite Science and Technology*, 54(3):275–285, 1995.

[30] A. Puck and H. Schrmann. Failure analysis of frp laminates by means of physically based phenomenological models. *Composites Science and Technology*, 58(7):1045–1067, 1998.

[31] A. Puck and H. Schrmann. Failure analysis of frp laminates by means of physically based phenomenological models. *Composites Science and Technology*, 62(12):1633–1662, 2002.

[32] P. Raghavan and S. Ghosh. A continuum damage mechanics model for unidirectional composites undergoing interfacial debonding. *Mechanics of Materials*, 37(9):955–979, 2005.

[33] R. A. Schapery. A theory of mechanical behavior of elastic media with growing damage and other changes in structure. *Journal of the Mechanics and Physics of Solids*, 38(2):215–253, 1990.

[34] J. H. A. Schipperen. An anisotropic damage model for the description of transverse matrix cracking in a graphite-epoxy laminate. *Composite structures*, 53(3):295–299, 2001.

[35] R. Talreja and A. Cardon. A synergistic damage mechanics approach to durability of composite material systems. In H. Fukuda and K. Reifsnider, editors, *Progress in Durability Analysis of Composite Systems*, pages 117–129. A.A. Balkema, Rotterdam, Netherlands, 1996.

[36] X. S. Tang, C. P. Jiang, and J. L. Zheng. Anisotropic elastic constitutive relations for damaged materials by application of irreversible thermodynamics. *Theoretical and Applied Fracture Mechanics*, 38(3):211–220, 2002.

[37] S. W. Tsai and E. M. Wu. A general theory of strength for anisotropic materials. *Journal of composite materials*, 5(1):58–80, 1971.